Biomedical Signal Processing and Control 18 (2015) 325–333

Contents lists available at ScienceDirect

Biomedical Signal Processing and Control

journal homepage: www.elsevier.com/locate/bspc

On the use of high-order cumulant and bispectrum for muscular-activity detection

Eugenio Orosco[a,*], Pablo Diez[b], Eric Laciar[b], Vicente Mut[a], Carlos Soria[a], Fernando di Sciascio[a]

[a] UNSJ-CONICET, Instituto de Automática, Av. San Martin oeste 1109, J5400ARL San Juan, Argentina
[b] Gabinete de Tecnología Médica (GATEME), Facultad de Ingeniería-Universidad Nacional de San Juan (UNSJ), San Juan, Argentina

ARTICLE INFO

Article history:
Received 5 August 2014
Received in revised form 29 January 2015
Accepted 13 February 2015

Keywords:
EMG
HOS
Cumulants
Bispectrum

ABSTRACT

The electromyographic (EMG) signals are extensively used on feature extraction methods for movement classification purposes. High-order statistics (HOS) is being employed increasingly in myoelectric research. HOS techniques could be represented in the frequency domain (high-order spectra, e.g., bispectrum, trispectrum) or in the time domain (higher-order cumulants). More calculus is required for computing the HOS in the frequency domain. On the one hand, classical bispectrum-based features were applied to EMG signals. We propose novel third-order cumulant-based features for EMG signals. Three different classifiers are implemented for muscular-activity detection. Different analysis and evaluations were applied to both HOS-based features in order to qualify and quantify similarities. Based on these results, it is possible to conclude that cumulant-based features and bispectrum-based features had comparable behavior and allowed similar classification rates. Hence, extra calculus in order to convert time- to frequency-domain should be avoided.

© 2015 Elsevier Ltd. All rights reserved.

1. Introduction

Muscular activity produces an electrical manifestation associated with the force and contraction level. This manifestation is known as electromyographic (EMG) signal and, can be acquired from the skin surface on a non-invasive way [1,2]. The understanding of EMG signals allows the comprehension of muscular activity, neuromuscular disorders and motion intentionality. Moreover, several physiological and anatomical factors, as well as the recording situations and the complexity of the signals are factors that justify a broad EMG signal processing field. These signals are used as reference inputs to myoelectric control systems. In these systems, there are two main areas related to the signal processing: the feature extraction and the classification of the EMG signals.

The digitalized EMG signals are large-dimension stochastic processes and the feature extraction techniques must reduce this dimensionality to a smaller dimensional space (the set of features). Ideally, features should be simple to extract, invariant to irrelevant transformations, insensitive to noise, and useful for characterizing and discriminating patterns [3]. The abstraction provided by a correct feature representation of the EMG signals allows the use of independent classification theory. Many feature extraction methods for EMG classification purposes have been reported [4]. The features can be grouped according to their domain (time [5], frequency [6], or time-frequency [7]), to the nature of the feature extraction mapping (linear or nonlinear [8,9]) or whether the feature extraction method is based on second or high-order statistics (HOS).

Classical researches on EMG activity detection methods have proposed techniques using single-threshold [10], double-threshold [11] and wavelet-MUAP [12] methods. Entropies have been used for EMG activity detection as well [13,14]. These researches have not used HOS techniques for EMG activity detection. HOS techniques are blind to additive colored or white Gaussian noise [15,16]. HOS have been applied in communications and sonar fields to detect random Gaussian signals in non-Gaussian noise or the opposite problem (non-Gaussian signals on Gaussian noise) [17,18]. It is pointed out that there are works in the field of EMG activity detection, and on the field of detection with HOS techniques but there is no information in the conjunction of areas.

Particularly, in the last years, the HOS techniques become relevant in the EMG pathologies and movement classification. The modeling of non-Gaussian and non-linear signals is one of the elemental approaches of HOS, as pointed out by Nikias et al.

* Corresponding author. Tel.: +54 264 4213303.
E-mail address: eorosco@inaut.unsj.edu.ar (E. Orosco).

http://dx.doi.org/10.1016/j.bspc.2015.02.011
1746-8094/© 2015 Elsevier Ltd. All rights reserved.

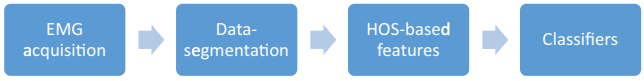

Fig. 1. General scheme of muscular activity detection using HOS-based features. EMG signal acquisition based on an experiment protocol is the first stage. Following, data are segmented and HOS-based features are calculated. Finally, muscular activity detection is performed by classifiers.

[15,16] and Swami et al. [19] (more extensive theoretical works are presented in [20–24]). It is well-known that HOS domain representations are the cumulant sequences (time domain) and the polyspectra (frequency domain). Some authors have used the cumulant sequences to classify movements with diverse results [25], and to estimate the amplitude and the number of motor unit action potentials (MUAPs) [26]. On the other hand, the bispectrum (third-order polyspectra) has been used in more diverse ways. For instance, the relationships between the bicoherence (normalized bispectrum) and the force level were analyzed [27]. In [28–30] the MUAPs were estimated by the third-order spectrum and; the off-line hand movement classification based on bispectrum EMG signals was presented in [31,32]. In previous work done by this group, the problem of HOS-based feature classification on myoelectric control scheme was addressed [33,34].

It is important to note that the bispectrum is a bi-dimensional complex function represented by a complex matrix. Therefore, in order to perform a classification stage, this 2D complex array must be reduced into a real feature vector. Generally, the feature vectors were integrations over bi-frequency segments [31], bispectrum module mean over bi-frequency domain [32], and Pythagorean means from the module or the real component of the bispectrum matrix [33,34]. These feature vectors were proposed and analyzed under classification performance criteria, and results between 90% and 97% were reported.

In summary, the bispectrum is reduced into a small set of features achieving acceptable results. In previous work, authors analyzed the HOS estimation problems and then, an HOS-based myoelectric control scheme was implemented. Essentially, the third order cumulant sequences and the bispectrum provide the same information in two different domain representations. Here, it raises the question of how much the classification rate increases/decreases while working with HOS on the frequency- or on the time-domain.

In this work, a comparison between a bispectrum-based feature and a cumulant-based feature is proposed. The EMG signal binary classification or detection problem is addressed as a practical procedure of comparison. Thus, the hypothesis of similar results achieved by the bispectrum- or cumulant-based features is verified. This is important in order to avoid extra calculus, i.e., the transformation from time- to frequency-domain is not needed in these applications.

The paper is organized as follows: Section 2 explains the experimental procedure for EMG signal acquisition, processing, and classification. Authors also provide a brief overview of data segmentation, surface electromyogram models, cumulants and bispectrum definitions, and HOS-based features extraction. Section 3 presents and discusses results in relation to similar performance of the cumulant-based features and the bispectrum-based features. Finally, Section 4 states the conclusions. The HOS estimation methods are presented in Appendix A.

2. Materials and methods

The EMG feature extraction methods based on third-order cumulants and bispectrum are described in this section. The block diagram of the overall processing scheme is shown in Fig. 1. The development of this section is based on this diagram.

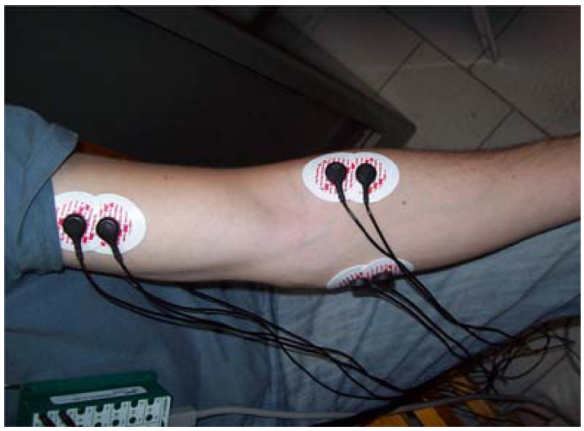

Fig. 2. A movement-based protocol is designed for recording the upper limb EMG signals for *biceps brachii*, *triceps brachii* (occluded in picture), *pronator* and *brachioradialis* muscles. The movements of interest in this work are flexion, extension, pronation, supination, and rest position.

2.1. Experimental protocol, front-end processing and EMG acquisition

A movement-based protocol is designed for recording the upper limb EMG signal from *biceps brachii*, *triceps brachii*, *pronator* and *brachioradialis* muscles (Fig. 2). The movements addressed in this work are flexion, extension, pronation, supination, and rest position. The volunteers are encouraged to perform the sequence of movements prompted by beepers. The database consists of the records of six volunteers, three male and three females, volunteers aged 28.6 ± 5.4, height 1.77 ± 0.13 m and weight 66.2 ± 12.7 kg. All volunteers are healthy, with no history of muscle weakness, neurological diseases or drug therapy. One of them has a congenital malformation, i.e., unilateral phocomelia below elbow (Vol 1); moreover, this volunteer had participated in other experimental myoelectric systems. The volunteers have approved and signed an informed consent form, according to the experiments to be performed.

The database was collected in four experimental trials, completed on four different days in order to avoid muscular fatigue [4]. Each trial consisted of five series of sequential movements, holding each motion for three seconds and interspersing the rest position. Each trial has 120 s maximum duration. The signals were grouped by an expert in agonist EMG signals. All these signals segments had sub-segments of non-activity and muscular activity.

The commercial data acquisition system is a 15LT – Grass Technologies®. Signals are sampled at 1 kHz with a 16-bit A/D converter (National Instruments DAQPad-6015). The EMG signals from four channels were registered by the data acquisition systems.

2.2. Data segmentation

The idea behind data segmentation is that the signal can be considered quasi-stationary during these time intervals; then, the data can be processed 'batch-wise' from segment to segment. A time segment is a time interval used to acquire myoelectric data needed for some kind of signal processing, such as detection. A trade-off balance between the accuracy of the classification and the response time can be determined by the segment length. In this work a segment length of 256 samples was adopted according to time constraints of the myoelectric control application [4,35]. The percentage of overlapping affects the rate at which class decisions

are updated. If the detection problem is the goal of the classification, this amount should be small enough to detect the EMG activity as fast as it could. Here, a 12.50% overlapping (32 samples) is experimentally adopted to obtain a continuous classification scheme.

2.3. HOS-based features

In this section a background of EMG and HOS is introduced. Then, the cumulants and bispectrum are defined. Finally, the feature extraction based on both methods is proposed.

2.3.1. Background on EMG models and HOS

The surface EMG signal can be commonly modeled by a bandwidth-limited, correlation-ergodic, centered (zero-mean) Gaussian process, modulated by muscular activity and corrupted by additive Gaussian white noise [36], Laplacian process [37] or Gaussian mixture models [38]. The sample or empirical marginal probability density function (PDF) of EMG signal amplitudes has investigated by several authors [39–43].

The HOS of a random process is identically zero when their joint PDFs are symmetric. The bispectrum vanishes when their marginal PDF are symmetric [44,45] only for the special case where the process is white. To the contrary, the joint PDFs must be null in order to verify that a zero-mean, stationary random process has identically zero third-order statistics, as was pointed out in [34]. Because it is well-known that the EMG signal is not white, the symmetry of the marginal PDF of the EMG signals by itself is insufficient to conclude that the third-order statistics are zero.

Recently, Ayachi et al. proposed a complex and complete EMG signal model applied to classify three contraction levels [46]. This very interesting research analyzed the PDFs shape based on HOS parameters (skewness and kurtosis) and core shape modeling (CSM). They concluded that shape modifications occur in sEMG amplitude distributions with varying muscle activation intensity. This clearly justifies the use of EMG cumulant and bispectrum features for movement classification tasks.

2.3.2. Cumulants and bispectrum definitions

The third-order cumulant sequences are high-order correlations (time-domain) and the bispectrum is a third-order frequency-domain measure. These HOS techniques contain information that conventional correlation and spectral analysis techniques cannot provide [15,16,19,47]. This is especially useful for non-Gaussian and non-linear signals, as the EMG. In the following, the definitions and some basic properties are recalled.

Let $\{X(k)\}$, $k = 0, 1, 2, 3, \ldots$ be a real stationary discrete time random process whose first n-moment exists. Then, the n-moment function [47] can be defined as

$$m_n^x(\tau_1, \tau_2, \ldots, \tau_{n-1}) = E\{X(k)X(k+\tau_1)\cdots X(k+\tau_{n-1})\} \quad (1)$$

where $E\{.\}$ is the statistical expectation and τ_i is the time shift. The most widespread moment functions are: the second moment or autocorrelation function $m_2^x(\tau)$, the third-order moment functions $m_3^x(\tau_1, \tau_2)$ and the fourth-order moment function $m_4^x(\tau_1, \tau_2, \tau_3)$.

For $n = 1, 2$ and 3 the general relationship between moments and cumulant functions are given by

$$c_1^x = m_1^x = E\{X(k)\} \quad (2a)$$

$$c_2^x(\tau_1) = m_2^x(\tau_1) - (m_1^x)^2 = m_2^x(-\tau_1) - (m_1^x)^2 = c_2^x(-\tau_1) \quad (2b)$$

$$c_3^x(\tau_1, \tau_2) = m_3^x(\tau_1, \tau_2) - m_1^x[m_2^x(\tau_1) + m_2^x(\tau_2) + m_2^x(\tau_1 - \tau_2)] - 2(m_1^x)^3 \quad (2c)$$

where c_1^x is the mean value of $\{X(k)\}$ and c_2^x is the auto-covariance sequence. The third-order cumulant function is $c_3^x(\tau_1, \tau_2)$ and, when the random sequence $\{X(k)\}$ is zero mean, the cumulant function is equivalent to the moment function, that is,

$$m_3^x(\tau_1, \tau_2) = c_3^x(\tau_1, \tau_2) = E\{X(k)X(k+\tau_1)X(k+\tau_2)\} \quad (2d)$$

Important properties justify the use of cumulants instead of moments [15,16]. First, high-order cumulant functions extract information deriving from deviations from Gaussianity. Second, the polyspectra of the white noise is a multidimensional flat function. Third, the cumulant functions of two statistically independent random processes are equal to the sum of the individual cumulant functions of each process. Therefore, the cumulant functions can be treated as an operator and consequently, the discrete time Fourier transform (DTFT) is applicable.

Assuming that $c_3^x(\tau_1, \tau_2)$ is absolutely summable [47], the third-order spectra or the bispectrum can be defined as the two-dimensional DTFT of the third-order cumulant $c_3^x(\tau_1, \tau_2)$ as follows.

$$B_3^x(\omega_1, \omega_2) = \sum_{\tau_1=-\infty}^{\infty}\sum_{\tau_2=-\infty}^{\infty} c_3^x(\tau_1, \tau_2)\exp\{-j(\tau_1\omega_1 + \tau_2\omega_2)\} \quad (3)$$

where $|\omega_1| \le \pi; |\omega_2| \le \pi; |\omega_1 + \omega_2| \le \pi$ and $c_3^x(\tau_1, \tau_2)$ is the third-order cumulant function of the random sequence $\{X(k)\}$. Symmetries in third-order cumulants function and the corresponding bispectrum function can be found in [15,47].

The estimation methods for the third-order cumulant and the bispectrum are detailed in Appendix A. Summarizing these methods, the third-order cumulant-based feature from the EMG signals over the sliding time windows were calculated. The EMG segment was divided into two groups of 128 samples. The third-order cumulants of each group was calculated (considering the symmetry properties). Finally, the cumulant of the EMG segment was the average of the cumulant groups. The bispectrum function was calculated as the DTFT of the third-order cumulant sequences. The bispectrum estimation results in a complex square matrix.

2.3.3. Feature extraction

The bispectrum-based features based on the bispectrum module and slight modifications are commonly used by several authors [27,31–34]. The third-order cumulant sequences and the bispectrum provide the same information in two different domain representations. Therefore, similar features could be extracted from third-order cumulant. Consequently, two cumulant-based features are introduced, as novel approaches. These features are based on the third order cumulant module. The innovative approach is that cumulants are simpler to extract than bispectrum, as is depicted in Fig. 3. The features were computed as:

Bispectrum-based feature: Two features were extracted from the bispectrum module. The first one (Eq. (4a)) is calculated over all frequency domain. This feature was proposed in our previous work [33,34]. The second one (Eq. (4b)) discards the diagonal slide as in other HOS work [32].

$$AM\hat{B}_3^x = \left(\frac{1}{M^2}\sum_{i=1}^{M}\sum_{j=1}^{M}\left|\hat{B}_3^x(i,j)\right|\right)^{1/4} \quad (4a)$$

$$AMD\hat{B}_3^x = \left(\frac{1}{M^2}\sum_{i=1}^{M}\sum_{j=1}^{M}\left|\hat{B}_3^x(i,j)\right|\right)^{1/4} \quad i \neq j \quad (4b)$$

where x is EMG data segment and M is size of the square matrix of bispectrum.

Third-order cumulant-based feature: Two novel features are introduced as the arithmetic mean of the third order cumulant module. The first one (Eq. (5a)) is calculated over all time domain

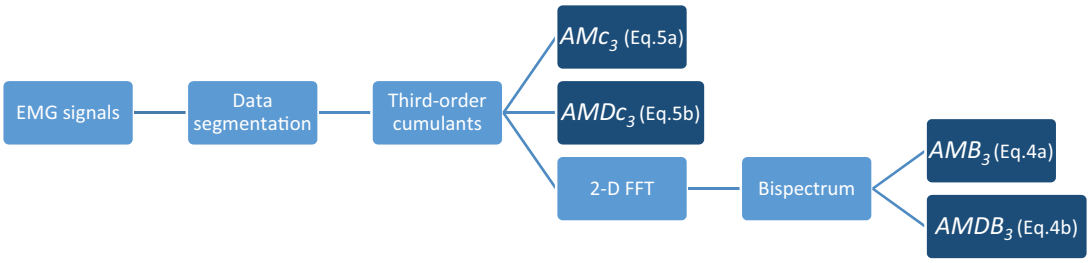

Fig. 3. Feature vectors calculated from the third-order cumulants and bispectrum. The diagram exposes the processing based on HOS features using: third-order cumulants and bispectrum.

and the second (Eq. (5b)) discards the diagonal slide in concordance to [32].

$$AM\hat{c}_3^x = \left(\frac{1}{M^2} \sum_{i=1}^{M} \sum_{j=1}^{M} \left| \hat{c}_3^x(i,j) \right| \right)^{1/4} \tag{5a}$$

$$AMD\hat{c}_3^x = \left(\frac{1}{M^2} \sum_{i=1}^{M} \sum_{j=1}^{M} \left| \hat{c}_3^x(i,j) \right| \right)^{1/4} \quad i \neq j \tag{5b}$$

Note, that the feature extracted from bispectrum according to Eq. (4a) is similar to the feature extracted by Eq. (5a) from the third-order cumulant (identically for Eqs. (4b) and (5b)).

The features described in Eqs. (5a) and (5b) are calculated over all time domain, i.e., using the entire Cumulant matrix. Moreover, the module and the quarter-root were applied to the cumulants in order to achieve more peaked feature's probability distribution, which has better numerical properties [33]. According to the authors' knowledge, these time features have not been used in the related bibliography.

2.4. Classification method

Several classifiers have been used for EMG classification. For example, different artificial neural networks, support vector machines, multiple classifiers with competence function, linear Bayesian classifier, and so on.

It is well established [3,4] that the feature extraction from EMG signals is the main kernel of classification system, so the success of any pattern recognition problem depends almost entirely on the selection and extraction of features. In this work, three classifiers for detection of muscular activity were used: artificial neural network (ANN), support vector machines (SVM) and linear discriminant analysis (LDA).

A feed-forward neural network was used because of, among other things, its great simplicity, straightforward numerical implementation, acceptable classification rate, and good performance. This ANN has one hidden layer and one output layer. The hidden layer contains 20 neurons and the output layer has one neuron, both layers with hyperbolic tangent sigmoid activation function. The selection of the number of hidden neurons has been determined directly by minimizing the combination of squared errors and weights, and by maximizing the classification rate [48]. A Bayesian regularization algorithm [49,50] was used for neural network training. This method uses a modified performance function, which is designed to minimize over-training, and to obtain a classifier with improved generalization properties.

SVM is another tool used for the classification of EMG movements and muscular activity detection. The SVM map input vectors into a higher dimensional space where the classification can be easily performed. Then SVM finds a linear separating hyperplane with the maximal margin in this higher dimensional space.

Given a training set of instance-label pairs $(x_i; y_i)$; $i = 1, \ldots, l$ where $x_i \in \Re^n$ and $y_i \in \Re^l$ such that $y_i \in \{1, -1\}$, the SVM require the solution of the following optimization problem:

$$\begin{aligned} \min_{w,b,\xi} \quad & \frac{1}{2} w^T w + C \sum_{i=1}^{l} \xi_i \\ \text{subject to} \quad & y_i(w^T \phi(x_i) + b) \geq 1 - \xi_i \\ & \xi_i \geq 0 \end{aligned} \tag{6}$$

where C is the penalty parameter of the error term ξ_i. The kernel function used in this work is a radial basis function on the form:

$$K(x_i, x_j) \equiv \phi(x_i)^T \phi(x_j) = e^{-\gamma \left\| x_i - x_j \right\|^2}, \quad \gamma > 0 \tag{7}$$

Therefore, the implementation of a SVM is needed to determine the parameters C and γ. The searching of C and γ is conducted through a grid-search using cross-validation [51]. The SVM used in this work is the one implemented in LIBSVM [52].

Finally, the LDA was implemented to evaluate the HOS-based features by means of a linear method. LDA is a linear combination of variables which must fill some requirements such as the "multivariate normality" (i.e., variables are normally distributed) [53,54]. The HOS-based features were not normally distributed; consequently, a logarithmic transformation was applied to the variables prior to LDA [55].

The Di Fabio's algorithm is a common technique used for comparison purpose on muscular activity detection [10]. The method used a threshold calculated as three-times the standard deviation above the mean value of the EMG in resting state. Besides, the signal must surpass the threshold during a whole period, to reduce false positive detections. In this work, the period was set at 32 ms. Both conditions were empirically selected to obtain the best results.

The results are reported using hold-out cross-validation scheme. In this sense, the features were randomized and the entire dataset was split in two halves. Then, both classifiers were trained in the first half and evaluated in the second one and vice versa. Finally, the classification performance is the average of both results.

3. Results and discussions

The third-order cumulants and bispectrum features herein proposed were experimentally evaluated. As was previously mentioned in Section 2.1, the EMG signals were grouped into segments of non-activity and muscular activity. From these segments, the continuous data segmentation was applied and Eqs. (4a), (4b), (5a), and (5b) were calculated. This process is depicted in Fig. 4.

Fig. 5 exposes the time evolution of the features according to Eqs. (4a) and (5a). The other two features (Eqs. (4b) and (5b)) were not shown due to minimal differences on graphics. The observed patterns on both features denote the presence of similarities, which

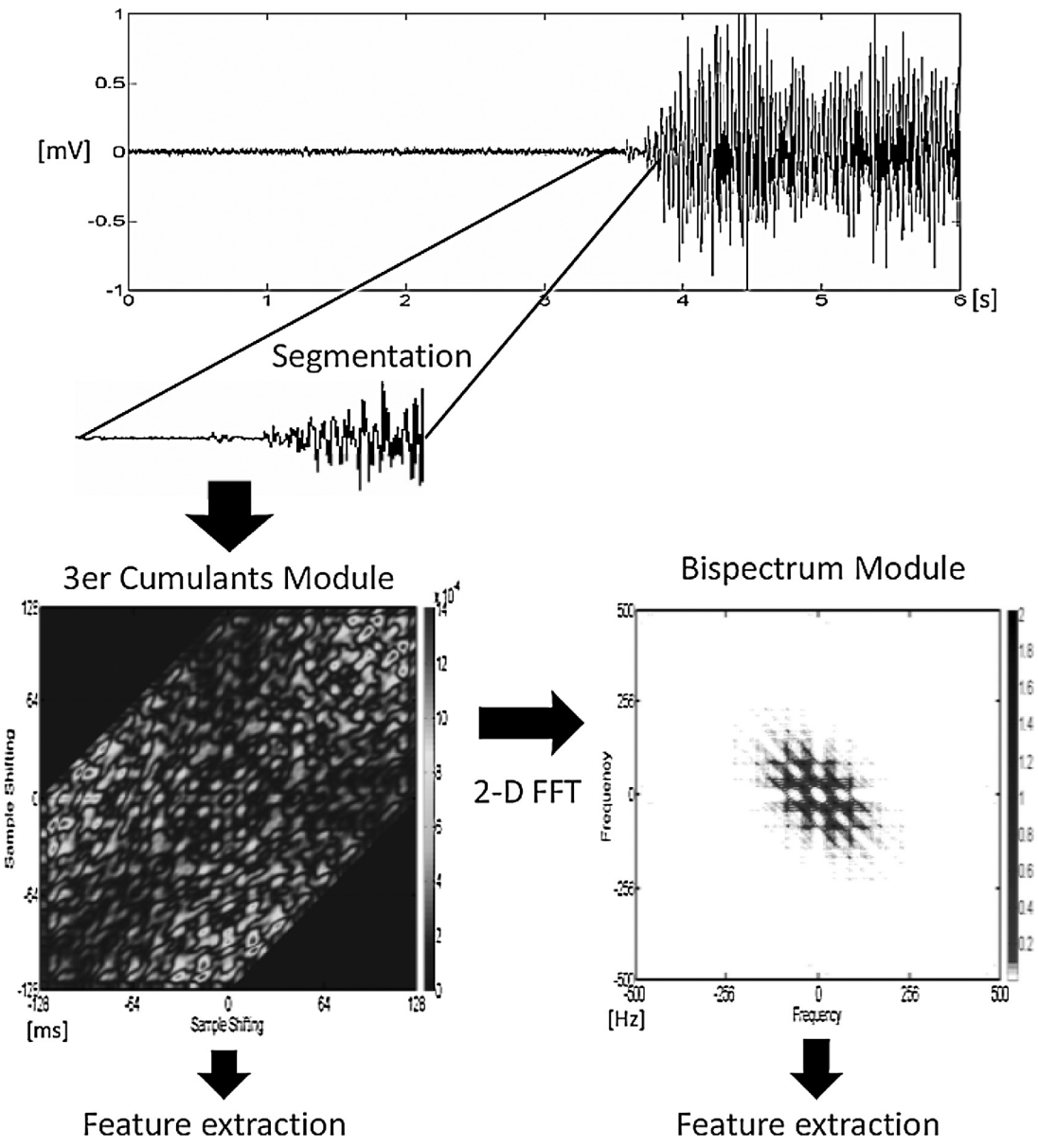

Fig. 4. HOS-based feature extraction. An EMG signal with non-activity and muscular activity was segmented. From this segment, the third-order cumulant and the bispectrum modules were calculated. Finally, the HOS-based features were computed.

clearly shows non-activity and activity feature patterns. Although, close similarities between time- and frequency-domain features are evident, a quantitative analysis is needed. Hence, the lineal correlation among the feature time series was measured in terms of the well-known Pearson's correlation and the coefficient of determination R^2.

The Pearson's correlation (r) is a measure of the linear association (correlation) between two variables or time series. It was evaluated in pairs taken from the four features. Table 1 summarizes the minimum and maximum values obtained along the six volunteers. A value $r = 1$ indicates a perfect correlation. In Table 1, the r values are close to 1 indicating a high level of correlation between the features. Another commonly used measure is the coefficient of determination (R^2), which is calculated as the square of r. The R^2 value indicates the ratio of the variance shared between two time series, e.g., an $R^2 = 0.7$ suggests that 70% of the variance is shared. In other words, 70% of the behavior of a variable could be described by the behavior of the other variable. Fig. 6 presents the average R^2 values and the corresponding standard deviation evaluated between the four features. An average R^2 of 0.9 ± 0.03 between the features is observed. Thus, similarities among the four features are verified. Moreover, a value close to 1 is obtained when evaluating features with and without the diagonal values, i.e., feature calculated with Eq. (4a) versus (4b) and with Eq. (5a) versus (5b). These results suggest that no significant differences are obtained by eliminating the diagonal values from the cumulant or bispectrum matrices.

The classification rate of the muscular activity detection was calculated using the EMG signals from the six subjects of the database. The ANN, SVM and LDA classifiers were implemented in order to evaluate the HOS-based features. Tables 2–4 exposed the correct classification rate for the three classifiers and for the four features (see Section 2.3.3). Average correct rate ranging from 90.4% up to 92.3% were reported for all classifiers. Subject 1 achieves the highest rates, possibly to his previous knowledge in myoelectric systems. On the other hand, Subject 2 has the poorest results.

Several results were obtained among the features; in some cases, higher rates were achieved using bispectrum features and in other cases, cumulant features allows obtaining higher results. However,

Table 1
Pearson's Correlation coefficients of the two bispectrum and the two third-order cumulant features time series.

	$AM\hat{B}_3^x$		$AMD\hat{B}_3^x$		$AM\hat{c}_3^x$		$AMD\hat{c}_3^x$	
	Max	Min	Max	Min	Max	Min	Max	Min
$AM\hat{B}_3^x$	×	×	0.9999999	0.9999972	0.9700930	0.9334140	0.9700253	0.9332333
$AMD\hat{B}_3^x$	0.9999999	0.9999972	×	×	0.9700659	0.9330047	0.9699982	0.9328229
$AM\hat{c}_3^x$	0.9700930	0.9334140	0.9700659	0.9330047	×	×	0.9999995	0.9999982
$AMD\hat{c}_3^x$	0.9700253	0.9332333	0.9699982	0.9328229	0.9999995	0.9999982	×	×

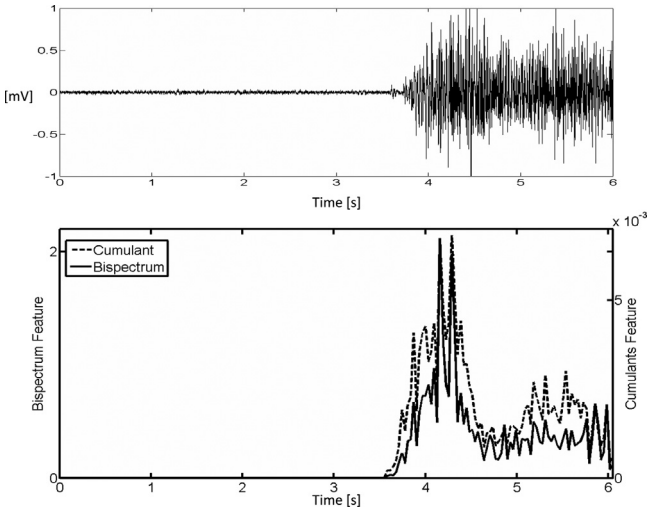

Fig. 5. Time evolution of the HOS-based features. Upper: an EMG signal of 6 s is shown. Lower: the features from third-order cumulant (right axes – dotted line) and bispectrum modules (left axes – straight black line) were computed over the time segments.

these differences in performance between time- and frequency-domain features are minimal. For example, the maximum drop rate is 1.1% when evaluating $AM\hat{B}_3^x$ against $AM\hat{c}_3^x$, using an ANN classifiers. Similar analysis in the results obtained with SVM and LDA showed a maximum drop rate of 0.5%. Note that, features with the diagonal slide and without it, reveal non-substantial changes on performances. This finding is in accordance with the r and R^2 values, suggesting that both variables contain the same information.

Additionally, Table 4 exposes the correct classification rates using the Di Fabio's method. This method achieved an average rate of 87.3%, which is lower than the proposed HOS-based method.

The differences (and similarities) in performance across the classifiers were evaluated by the Friedman test [56]. It is a non-parametric method, which can be applied to data classified by two (or more) criteria to determine its significant influence on the classification. Hence, the null hypothesis proposes that all the

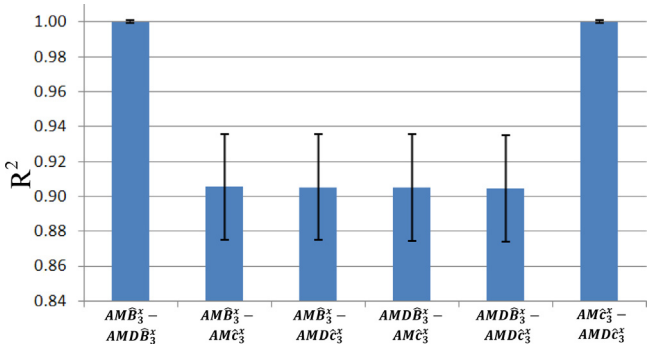

Fig. 6. Coefficient of determination (R^2). The average R^2 values and the corresponding standard deviation were evaluated in pairs taken from the four features.

Table 2
Correct classification rates of the two bispectrum and the two third-order cumulant features using an ANN classifier and cross-validation.

Subject	$AM\hat{B}_3^x$	$AMD\hat{B}_3^x$	$AM\hat{c}_3^x$	$AMD\hat{c}_3^x$
1	96.1%	96.0%	96.3%	96.2%
2	88.1%	85.9%	83.9%	85.5%
3	94.0%	93.7%	92.4%	92.8%
4	92.1%	92.1%	91.5%	91.7%
5	92.3%	92.1%	91.7%	91.4%
6	86.6%	86.0%	86.4%	89.9%
Average	91.5%	91.0%	90.4%	91.3%
SD	3.6%	4.1%	4.5%	3.5%

results are equivalent through the different features. The alternative hypothesis is that at least two results are different. Evaluating the results obtained with ANN (Table 2), the Friedman test reports a p-value of 0.241 ($\chi^2 = 4.2$; $N = 6$; d.o.f. = 3). In the case of results obtained with SVM (Table 3), the Friedman test reports a p-value of 0.073 ($\chi^2 = 6.96$; $N = 6$; d.o.f. = 3). The results obtained with LDA (Table 4) obtained a p-value of 0.046 ($\chi^2 = 8$; $N = 6$; d.o.f. = 3). In all cases, the null hypothesis cannot be rejected in favor of the alternative hypothesis. Therefore, authors can assume that the classification results are similar regardless of the used features.

In summary, the correlation results evidenced close similarity between the time-domain features and the frequency-domain features. Moreover, the classification results obtained with any of these features were similar.

Note that the binary classification of movements (non-activity against muscular activity) was presented and common and novel HOS-features were extracted. However, the HOS-based techniques could be useful in others areas, applications or even other pattern recognition schemes. For example, Ayachi et al. classified three contraction levels with minimal accuracy of 76% using k-means cluster based on HOS features (skewness and kurtosis) [46]. Another example proposed by Sezgin analyzed two contraction levels based on Bispectrum features achieving 97% of classification rate [32]. Both researches classified different contraction levels using time or frequency domain features. We verified the high correlation (Table 1 and Fig. 6) and similar behavior of time and frequency features (Fig. 5), therefore, it is expected that similar results could be achieved using Cumulant-based features instead of Bispectrum features. Note, however, that skewness is just one value of the Cumulant matrix ($c_3(0,0)$) and we used the entire Cumulant matrix.

Table 3
Correct classification rates of the two bispectrum and the two third-order cumulant features using an SVM classifier and cross-validation.

Subject	$AM\hat{B}_3^x$	$AMD\hat{B}_3^x$	$AM\hat{c}_3^x$	$AMD\hat{c}_3^x$
1	95.7%	95.7%	96.1%	96.2%
2	86.6%	86.6%	84.8%	84.9%
3	92.8%	92.8%	92.2%	92.1%
4	91.9%	91.8%	91.7%	91.7%
5	92.0%	92.0%	91.5%	91.7%
6	91.2%	91.2%	91.0%	91.1%
Average	91.7%	91.7%	91.2%	91.3%
SD	3.0%	3.0%	3.6%	3.6%

Table 4
Correct classification rates of the two bispectrum and the two third-order cumulant features using LDA classifier and cross-validation and single threshold (Di Fabio's technique).

Subject	$AM\hat{B}_3^x$	$AMD\hat{B}_3^x$	$AM\hat{c}_3^x$	$AMD\hat{c}_3^x$	Single threshold
1	95.7%	95.8%	95.6%	95.6%	90.9%
2	88.4%	88.4%	86.7%	86.7%	88.9%
3	94.0%	94.0%	93.4%	93.4%	93.4%
4	89.6%	89.6%	89.2%	89.2%	79.6%
5	92.1%	92.1%	91.7%	91.7%	85.4%
6	93.6%	93.6%	94.1%	94.1%	87.4%
Average	92.2%	92.3%	91.8%	91.8%	87.3%
SD	2.8%	2.8%	3.3%	3.3%	4.9

Other researchers have proposed different methods for EMG activity detection. For example, Zhou and Zhang proposed the onset detection on EMG signal using sample entropy and a threshold detector [14]. In a previous work of the authors, the sample entropy was applied to both, synthetic and real EMG signals [13]. Shannon introduced the entropy concept in 1948 [57]. Both HOS and entropy are non-parametric features. Entropy is easier to compute than HOS, but it only represents the average amount of information obtained from a measurement. Meanwhile, HOS can offer different and more varied information than entropy, as it is pointed out across this work and bibliography.

As was exposed by Merlo et al., EMG signal can be modeled as the summation of MUAPs and the Wavelet transform (WT) is suitable to analyze surface EMG because the MUAPs have the same shape but different width and amplitude [12]. A mother wavelet must be selected in order to apply the WT, moreover, the mother wavelet should be chosen according to the EMG detection modality. For example, Vannozzi et al. used Morlet mother wavelet [58]. Thus, Wavelet is a parametric method based on a structured model. In the opposite way, HOS are non-structured model-based and non-parametric. The foundation of the EMG models was introduced in Section 2.3.1. An advantage of HOS techniques over other methods is the well established immunity to Gaussian noise [15,16,47].

Generally, EMG activity detection has used simple classification algorithms, such as thresholds [10,11,13]. Instead, in pathologies and movement classification were used machine learning methods [5,7,9,27]. In the current work, three different methods were tested for EMG activity classification. Specifically, non-lineal and complex classifiers (SVM and ANN) and simple LDA classifier were evaluated. They achieved high accuracy across all the proposed features and moreover, no significant differences were reported among the classifiers. It was established that the feature extraction from EMG signals is the main kernel of classification system. In other words, the success of any pattern recognition problem depends almost entirely on the selection and extraction of features [3,4]. Hence, the similarities between cumulant-based and bispectrum-based features could be assumed by the similar classification rates independently of the classification method.

4. Conclusions

This paper presented a comparison between bispectrum-based features and cumulant-based features for muscular activity detection. Classical bispectrum-based features were computed and similar cumulant-based features were proposed. These features involved the basic operation of averaging the bispectrum module or third-order cumulant module (with and without considering the diagonal slide). As a practical experimental procedure, LDA, ANN and SVM classifiers detected non-activity against muscular activity.

The preliminary hypothesis of similar results was verified. There is no need on extra calculus of the transformation from time- to frequency-domain. In fact, acceptable classification rates are achieved when the bispectrum is reduced into a small set of features. Nevertheless, the third-order cumulant features also allow similar rates.

This similarity was addressed by proposing the 'rest-movement' classification. The application allowed qualifying and quantifying the similarity among two frequency-domain and two proposed time-domain features, that is the bispectrum- and the third-order cumulant-based features, respectively. Analysis of the classification rates, the Pearson's Correlation, the coefficient of determination and the Friedman test argued the principal hypothesis of this research.

Appendix A. Estimation methods

There are basically two approaches that have been used to estimate the HOS, namely, the parametric approach (which is based on linear parametric models, e.g., autoregressive (AR), moving average (MA), and ARMA models), and the 'Fourier type' approach [47]. A review of the commonly used techniques can be found in [59–62], and references therein. The estimators based on the approximation of the definition given by (2d) and (3). It follows from this definition that the accuracy of bispectrum estimation depends mainly on the accuracy of the third-order cumulant estimates. It is also well-known that for a fixed number of data samples, the variance of these estimates is greater than the second-order cumulant estimates (autocorrelation function).

A.1. Arithmetic mean third-order cumulant estimator

The standard unbiased estimator of the third-order cumulant sequence is equivalent to using the sample mean estimator,

$$\hat{c}_3^x(m,n) = \frac{1}{N-\max(m,n)} \sum_{l=1}^{N-\max(m,n)} x(l)x(l+m)x(l+n) \tag{A.1}$$

where in our case $X_N = \{x(k),\ k = 1, 2, ..., N\}$ is the EMG sequences (time segment) of $N = 2^8 = 256$ samples, $l = 1, 2, \ldots$ is the index of the sample segment, and $m = 0, 1, 2, \ldots, n = 0, 1, 2, \ldots$ are the time lags. Evidently, between l, m, n and N it must be satisfied the relation $1 \le \max(l+m, l+n) \le N$. Therefore, index l varies from 1 to $N - \max(m, n)$.

Eq. (A.1) can be written in a compact form as:

$$\hat{c}_3^x(m,n) = \frac{1}{K}\sum_{l=1}^{N-m} z_{m,n}(l) \tag{A.2}$$

where $z_{m,n}(l) = x(l)x(l+m)x(l+n)$ is defined for fixed values of m and n over the triangular region $m = 0, 1, 2, \ldots$ and $0 \le n \le m \le N-1$, the index l ranges from 1 to $N-m$, and K takes the values $N-m$ or N for unbiased or asymptotically unbiased estimator respectively.

In order to obtain an acceptable trade-off between the bias of the estimator and its variance, an ensemble (or time segments) averaging is used. This is a standard statistical technique used in the analysis of stationary time series. The finite sequence $X_N = \{x(k),\ k = 1, 2, ..., N\}$ is divided into D non-overlapping subsequences, each one having a length of M samples, such that $N = D \times M$. If $x^{(i)}(j), j = 1, 2, \ldots, M, i = 1, 2, \ldots, D$ denote the $k = (i-1)M + j$th observation in the original sequence, then the subsequences $X^{(i)}$ are defined as, $X^{(i)} = \{x^{(i)}(j) = x((i-1)M + j), j = 1, 2, \ldots, M\}, i = 1, 2, \ldots, D$.

Thus, the following ensemble average version of the estimator defined previously is calculated as the ensemble average of the cumulant subsequences estimates on the segments.

$$\hat{c}_3^{x-D}(m,n) = \frac{1}{D}\sum_{i=1}^{D}\frac{1}{M-m}\sum_{l=1}^{M-m} z_{m,n}^{(i)}(l) \tag{A.3}$$

where $z^{(i)}_{m,n}(l) = x^{(i)}(l)x^{(i)}(l+m)x^{(i)}(l+n), i = 1, 2, \ldots, D$ are defined in each subsequence $X^{(i)}$ for fixed values of m and n over the triangular region $m = 0, 1, 2, \ldots, 0 \le n \le m \le M-1$, the index l varies from 1 to M.

A.2. Bispectrum estimates

As we have pointed out previously, the bispectrum estimation is an approximation of the definition (3), calculated as:

$$\hat{B}^x_3(\omega_1, \omega_2) = \sum_{m=-L}^{L} \sum_{n=-L}^{L} \hat{c}^x_3(m, n) w(m, n) \exp\{-j(\omega_1 m + \omega_2 n)\} \quad \text{(A.4)}$$

where $L \le M-1$. The cumulant symmetries and the properties of its two-dimensional fast Fourier transform should be considered in order to reduce the computational cost [15,16,47]. As in the case of conventional power spectrum estimation, a bidimensional window function $w(m, n)$ is used to find the smooth bispectrum estimates. Furthermore, it is well-known that the selection of the window function $w(m, n)$ affects the bias-variance trade-off in the bispectrum estimation. The bidimensional window function $w(m, n)$ must satisfy several conditions [47]. Among other things, the authors concluded that the bispectrum estimated with Sasaki window has the lowest bias, and that of Parzen window has the lowest variance. According to this the Parzen window function has been chosen.

References

[1] C. De Luca, Physiology and mathematics of myoelectric signals, IEEE Trans. Biomed. Eng. 26 (6) (1979) 313–325.
[2] C.J. De Luca, Surface Electromyography: Detection and Recording, Delsys, Inc., 2002.
[3] R.O. Duda, P.E. Hart, D.G. Stork, Pattern Classification, 2nd ed., Wiley-Interscience Publication, New York, 2001.
[4] M. Oskoei, H. Hu, Myoelectric control systems: a survey, Biomed. Signal Process. Control 2 (2007) 275–294.
[5] M. Zardoshti-Kermani, B. Wheeler, K. Badie, R. Hashemi, EMG feature evaluation for movement control of upper extremity prostheses, IEEE Trans. Rehabil. Eng. 3 (1995) 324–333.
[6] D. Roman-Liu, M. Konarska, Characteristics of power spectrum density function of EMG during muscle contraction below 30% MVC, J. Electromyogr. Kinesiol. 19 (2009) 864–874.
[7] X. Zhang, Y. Wang, R.P.S. Han, Wavelet transform theory and its application in EMG signal processing, Proc. IEEE Seventh Int. Conf. Fuzzy Syst. Knowl. Discov. 5 (8) (2010) 2234–2238.
[8] M. Kurzynski, T. Woloszynski, A. Wolczowski, Multiclassifiers with competence function applied to the recognition of EMG signals for the control of bio-prosthetic hand, in: Proceedings of the 9th International Conference on Information Technology and Applications in Biomedicine, ITAB 2009, 2009, pp. 1–4.
[9] P.K. Artemiadis, K.J. Kyriakopoulos, An EMG-based robot control scheme robust to time-varying EMG signal features, IEEE Trans. Inf. Technol. Biomed. 14 (3) (2010) 582–588.
[10] R.P. di Fabio, Reliability of computerized surface electromyography for determining of onset of muscle activity, Phys. Ther. 67 (1) (1987) 43–48.
[11] P. Bonato, T. D'Alessio, M. Knaflitz, A statistical method for the measurement of muscle activation intervals from surface myoelectric signal during gait, IEEE Trans. Biomed. Eng. 45 (1998) 287–298.
[12] A. Merlo, D. Farina, R. Merletti, A fast and reliable technique for muscle activity detection from surface EMG signals, IEEE Trans. Biomed. Eng. 50 (3) (2003) 316–323.
[13] N.M. López, E. Orosco, F. di Sciascio, Surface electromyographic onset detection based on statistics and information content, J. Phys.: Conf. Ser. 332 (2011) 1–9.
[14] P. Zhou, X. Zhang, A novel technique for muscle onset detection using surface EMG signals without removal of ECG artifacts, Physiol. Meas. 35 (2014) 45–54.
[15] C.L. Nikias, J.M. Mendel, Signal processing with higher-order spectra, IEEE Signal Process. Mag. 10 (3) (1993) 10–37.
[16] C.L. Nikias, M.R. Raghveer, Bispectrum estimation: a digital signal processing framework, Proc. IEEE 75 (7) (1987) 869–891.
[17] G.B. Giannakis, M.K. Tsatsanis, Signal detection and classification using matched filtering and higher order statistics, IEEE Trans. Acoust. Speech Signal Process. 38 (7) (1990) 1284–1296.
[18] B.M. Sadler, G.B. Giannakis, K. Lii, Estimation and detection in non-Gaussian noise using higher order statistics, IEEE Trans. Signal Process. 42 (10) (1994) 2729–2741.
[19] A. Swami, J.M. Mendel, C.L. Nikias, Higher-Order Spectral Analysis Toolbox for Use with Matlab, User's Guide, MathWorks Inc., 1998.
[20] M.B. Priestley, Spectral Analysis and Time Series, vol. I, 11th ed., Academic Press Inc., Great Britain, 1981, pp. 871–874.
[21] D.R. Brillinger, Time Series, Data Analysis and Theory, SIAM ed., Holden Day Inc., San Francisco, 2001 (chapter 2).
[22] D.R. Brillinger, Some history of the study of higher-order moments and spectra, Stat. Sin. 1 (1991) 465–476.
[23] D.R. Brillinger, An introduction to polyspectra, Ann. Math. Stat. 36 (5) (1965) 1351–1374.
[24] M.G. Kendal, The Advanced Theory of Statistics, vol. I, 2nd ed., Charles Griffin & Company Limited, London, 1945 (Ch. 3).
[25] K. Nazarpour, A.R. Sharafat, S.M. Firoozabadi, Application of higher order statistics to surface electromyogram signal classification, IEEE Trans. Biomed. Eng. 54 (10) (2007) 1762–1769.
[26] K. Kanosue, M. Yoshida, K. Akazawa, K. Fujii, The number of active motor units and their firing rates in volunteer contraction of human brachialiis muscle, Jpn. J. Physiol. 29 (4) (1974) 427–443.
[27] P.A. Kaplanis, C.S. Pattichis, L.J. Hadjileontiadis, V.C. Roberts, Surface EMG analysis on normal subjects based on isometric volunteer contraction, J. Electromyogr. Kinesiol. 19 (1) (2009) 157–171.
[28] S. Shahid, J. Walker, G.M. Lyons, C.A. Byrne, A.V. Nene, Higher order statistics techniques applied to EMG signal, IEEE Trans. Biomed. Eng. 52 (7) (2005) 1195–1209.
[29] K. Yana, H. Mizuta, R. Kajiyama, Surface electromyogram recruitment analysis using higher order spectrum Proceedings of the IEEE 17th Annual Conference Engineering in Medicine and Biology Society, vol. 2, 1995, pp. 1345–1346.
[30] E. Plévin, D. Zazula, Decomposition of surface EMG signals using non-linear LMS optimization of higher-order cumulants, in: Proceedings of the 15th IEEE Symposium on Computer-Based Medical Systems, 2002, pp. 5912–5915.
[31] X. Chen, X. Zhu, D. Zhang, A discriminant bispectrum feature for surface electromyogram signal classification, Med. Eng. Phys. 32 (2) (2010) 126–135.
[32] N. Sezgin, Analysis of EMG signals in aggressive and normal activities by using higher-order spectra, Sci. World J. 2012 (2012) 1–5, http://dx.doi.org/10.1100/2012/478952 (Article ID 478952).
[33] E.C. Orosco, N.M. Lopez, F. di Sciascio, Bispectrum-based features classification for myoelectric control, Biomed. Signal Process. Control 8 (March (2)) (2013) 153–168 (ISSN 1746-8094).
[34] E. Orosco, N. López, C. Soria, F. di Sciascio, Surface electromyogram signals classification based on bispectrum, in: Proceedings of the 2010 Annual International Conference of the IEEE of Engineering in Medicine and Biology Society (EMBC), 2010, pp. 4610–4613.
[35] K. Englehart, B. Hudgins, A robust, real-time control scheme for multifunction myoelectric control, IEEE Trans. Biomed. Eng. 50 (7) (2003) 848–854.
[36] E. Clancy, E. Morin, R. Merletti, Sampling, noise-reduction and amplitude estimation issues in surface electromyography, J. Electromyogr. Kinesiol. 12 (2002) 1–16.
[37] E.A. Clancy, N. Hogan, Multiple site electromyographic amplitude estimation, IEEE Trans. Biomed. Eng. 42 (2) (1995) 203–211.
[38] Y. Huang, K. Englehart, B. Hudgins, A. Chan, Optimized Gaussian mixture models for upper limb motion classification, IEEE Trans. Biomed. Eng. 52 (11) (2005) 1801–1811.
[39] E.A. Clancy, N. Hogan, Probability density of the surface electromyogram and its relation to amplitude detectors, IEEE Trans. Biomed. Eng. 46 (6) (1999) 730–739.
[40] K. Nazarpour, A.H. Al-Timemy, G. Bugmann, A. Jackson, A note on the probability distribution function of the surface electromyogram signal, Brain Res. Bull. 90 (2013) 88–91.
[41] A.S. Cherniz, C.E. Bonell, C.B. Tabernig, Study of the SEMG probability distribution of the paretic tibialis anterior muscle, J. Phys.: Conf. Ser. 90 (2007), http://dx.doi.org/10.1088/1742-6596/90/1/012054, 012054.
[42] G.R. Naik, D.K. Kumar, S.P. Arjunan, Kurtosis and negentropy investigation of myoelectric signals during different MVCs, in: ISSNIP Biosignals and Biorobotics Conference, 2011, pp. 1–4.
[43] K. Nazarpour, A.R. Sharafat, S.M. Firoozabadi, Negentropy analysis of surface electromyogram signal, in: IEEE/SP 13th Workshop on Statistical Signal Processing, 2005, pp. 974–977.
[44] M.R. Raghuveer, Higher-order statistics: laying a myth to rest Proceedings of the 28th Asilomar Conference on Signals, Systems and Computers, vol. 1, 1994, pp. 5–8.
[45] M.R. Raghuveer, Third-order statistics: issue of PDF symmetry, IEEE Trans. Signal Process. 43 (7) (1995) 1736–1738.
[46] F.S. Ayachi, S. Boudaoud, C. Marque, Evaluation of muscle force classification using shape analysis of the sEMG probability density function: a simulation study, Med. Biol. Eng. Comput. 52 (8) (2014) 673–684.
[47] C. Nikias, A. Petropulu, Higher-Order Spectral Analysis: A Nonlinear Signal Processing Framework, Prentice-Hall, Inc., New Jersey, 1993.
[48] B. Curry, P.H. Morgan, Model selection in neural networks: some difficulties, Eur. J. Oper. Res. 170 (2006) 567–577.
[49] D.J.C. MacKay, Bayesian interpolation, Neural Comput. 4 (3) (1992) 415–447.
[50] F.D. Foresee, M.T. Hagan, Gauss–Newton approximation to Bayesian regularization Proceedings of the International Joint Conference on Neural Networks, vol. 3, 1997, pp. 1930–1935.
[51] C.-W. Hsu, C.-C. Chang, C.-J. Lin, A Practical Guide to Support Vector Classification, Department of Computer Science, National Taiwan University, Taiwan, 2008, http://www.csie.ntu.edu.tw/ cjlin/papers/guide/guide.pdf (accessed 21.05.08).

[52] C.-C. Chang, C.-J. Lin, LIBSVM: A Library for Support Vector Machines, Department of Computer Science, National Taiwan University, Taiwan, 2008, Available from: http://www.csie.ntu.edu.tw/ cjlin/libsvm (accessed 21.05.08).
[53] H.E.A. Tinsley, S.D. Brown (Eds.), Handbook of Applied Multivariate Statistics and Mathematical Modeling, 1st ed., Academic Press, USA, 2000.
[54] J. Gil Flores, E. García Giménez, G. Rodríguez Gomez, in: S.A. La Muralla, S.I. Hespérides (Eds.), Books of Statistics No. 12: Discriminant Analysis, 2001 (in Spanish).
[55] R.L. Scheaffer, J.T. McClave, Probability and Statistics for Engineers, Editorial Iberoamericana, Mexico, 1993 (in Spanish from the 3rd edition in English).
[56] M. Friedman, The use of ranks to avoid the assumption of normality implicit in the analysis of variance, J. Am. Stat. Assoc. 32 (1937) 675–701.
[57] C.E. Shannon, A mathematical theory of communication, AT&T Tech. J. 27 (1948), 379–423, 623–656.
[58] G. Vannozzi, S. Conforto, T. D'Alessio, Automatic detection of surface EMG activation timing using a wavelet transform based method, J. Electromyogr. Kinesiol. 20 (2010) 767–772.
[59] P.J. Huber, Robust Statistics, John Wiley and Sons, New York, 1981.
[60] A.K. Nandi, Robust estimation of third-order cumulants in applications of higher-order statistics, IEEE Proc. Radar Signal Process. 140 (6) (1993) 380–389.
[61] K. Nandi, D. Mampel, Development of an adaptive generalized trimmed mean estimator to compute third-order cumulants, Signal Process. 57 (3) (1997) 271–282.
[62] Y. Zhang, D. Hatzinakos, A.N. Venetsanopoulos, Bootstrapping techniques in the estimation of higher-order cumulants from short data records 1993 IEEE International Conference on Acoustics, Speech, and Signal Processing, ICASSP-93, vol. 4, 1993, pp. 200–203.